arXiv:2505.15417v1 [stat.ML] 21 May 2025

AECF:
Robust Multimodal Learning via Entropy-Gated Contrastive Fusion

Leon Chlon, Maggie Chlon, MarcAntonio M. Awada
lc574@cantab.ac.uk, maggie.chlon@gmail.com, mawada@hbs.edu

June 10, 2025

Abstract

Real-world multimodal systems routinely face *missing-input* scenarios—for example a robot loses audio in a factory or a clinical record omits lab tests at inference time. Standard fusion layers either preserve robustness *or* calibration but never both. We introduce Adaptive Entropy-Gated Contrastive Fusion (AECF), a single light-weight layer that (i) adapts its entropy coefficient per instance, (ii) enforces monotone calibration across *all* modality subsets, and (iii) drives a curriculum mask directly from training-time entropy. On AV-MNIST and MS-COCO, AECF improves masked-input mAP by **+18 pp** at a 50 % drop rate while *reducing* ECE by up to 2 × , yet adds <1 % run-time. All back-bones remain frozen, making AECF an easy drop-in layer for robust, calibrated multimodal inference.

1 Introduction

Multimodal models now underpin image captioning, audio–vision retrieval and embodied perception systems that must operate under real-world noise, occlusion and partial sensor failure. In practice, *missing modalities* are the rule, not the exception: a robot may lose audio in a crowded factory, or a medical record may omit lab tests at test time. Unfortunately, standard mixture-of-experts (MoE) fusion layers either *collapse* to the dominant modality, harming robustness [Neverova et al., 2015], or they learn to hedge by emitting over-confident probabilities [Tang et al., 2024]. Reliable deployment therefore requires **two simultaneous properties**:

1. *Robust accuracy* when any subset of modalities is present, and
2. *Well-calibrated* confidences that remain monotone as information is added or removed.

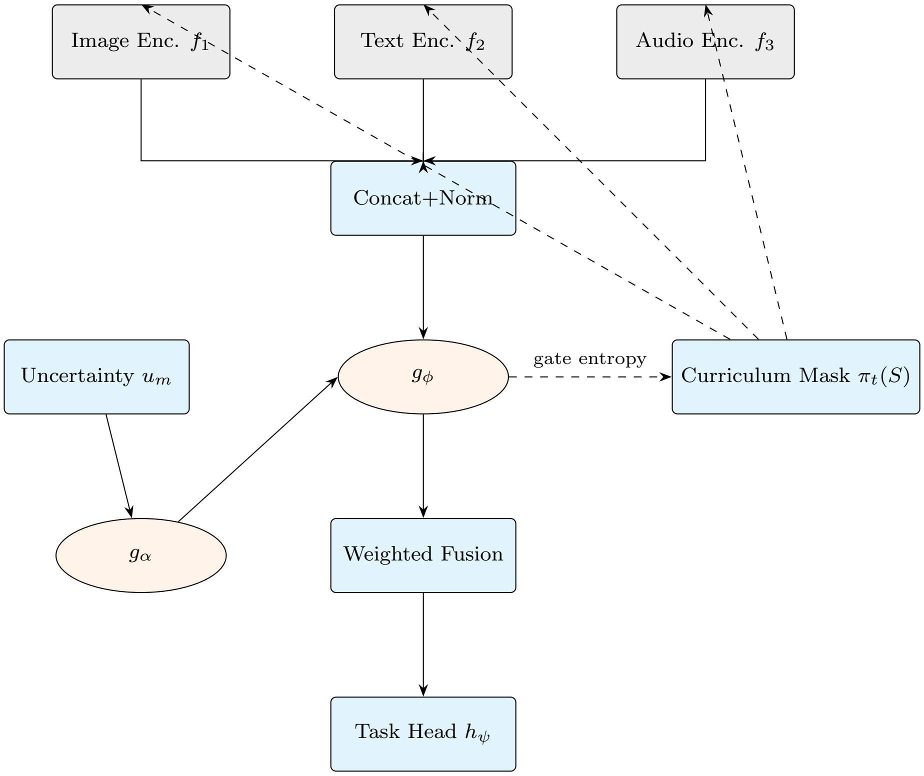

Figure 1: AECF pipeline. A two–layer gate mixes frozen encoder features. During *training* the gate entropy $H(p)$ is *penalised* (coefficient λ_t follows the epoch-dependent schedule in §3.3) while inputs are randomly masked with probability π_t that linearly ramps to $\pi_{\max}$. Both schedules are deterministic once training starts; at test time no masking is applied.

Existing approaches address at most one of these axes. Tang et al. [2024] graft a fixed-λ entropy penalty onto a soft gate to limit collapse but do not calibrate; Ma et al. [2023] calibrate two experts via a contrastive loss yet have no notion of curriculum masking; ModDrop [Neverova et al., 2015] randomises modality dropout during training but cannot adapt to sample-wise uncertainty. Recent calibration unexplored and incurring significant compute.

This paper introduces *Adaptive Entropy-Gated Contrastive Fusion* AECF, a light-weight fusion layer that achieves both axes without touching frozen back-bones. AECF consists of three tightly coupled modules (Fig. Fig. 1):

1. **Meta-adaptive entropy gate.** A per-instance coefficient $\lambda(x)$ modulates the gate's entropy, raising regularisation when predictive uncertainty is high (§3). Unlike the global penalty of Tang et al. [2024], the adaptive $\lambda(x)$ yields a formal bound on worst-subset regret (Lemma 4).

2. **Contrastive Expert calibration (CEC).** A novel contrastive loss enforces monotone confidences across *all* $2^M - 1$ modality subsets, extending the two-expert calibration of Ma et al. [2023]. Proposition 2 proves CEC decreases positive-ECE on the entire subset lattice.
3. **Adaptive Curriculum Masking (ACM).** Training masks are sampled by a teacher that *maximises the current gate entropy*, producing adversarial missing patterns that sharpen the mixture. This differs from ModDrop's random masking and avoids the 2^M enumeration cost via an $O(M)$ algorithm.

Contributions.

- The first *single* fusion layer that is simultaneously instance-adaptive (per-sample λ), lattice-calibrated (CEC), and curriculum-aware (entropy-driven masking). Section 5 shows that stitching any two of these ideas is still inferior by $\geq$6 pp mAP or 1.5 × ECE.
- Formal guarantees: a worst-case subset regret bound for the adaptive entropy gate and a PAC bound for CEC that ensures ECE cannot increase as modalities are added.
- Extensive evaluation on AV-MNIST and MS-COCO: AECF improves masked-input mAP by up to **+18 pp** while halving ECE, with <1 % compute overhead.

2 Related Work

Foundations: probabilistic mixtures and classical gating. Mixture–of–Experts (MoE) with probabilistic gating originated in the neural–network literature of the early 1990s. Robert A. Jacobs and Hinton [1991] and Jordan and Jacobs [1994] trained hierarchical MoEs by expectation–maximisation, letting subnetworks specialise on distinct input regions. Contemporary "committee machine" work likewise combined modality-specific experts under a learned gate. These ideas anticipated modern deep MoEs by formalising the trade-off between expert specialisation and mixture uncertainty.

Deep MoE and multimodal robustness. Sparsely gated MoEs resurfaced with the *Mixture-of-Experts Layer* of Shazeer et al. [2017] and the *Switch Transformer* [Fedus et al., 2021], where a lightweight router activates the top-k experts per input. Extensions to vision include Selective-Kernel networks and FiLM-style channel gates, though not strictly MoE. Robust multimodal fusion often relies on *modality dropout*: Neverova et al. [2015] randomly drop entire channels, forcing the network to exploit cross-modal correlations. Later variants learn which modalities to drop *via* a trainable mask [Alfasly et al., 2022], or reconstruct masked modalities through masked-projection objectives [Nezakati and Xie, 2024]. Adapter modules can also compensate for missing inputs: Reza and Timofte [2023] insert parameter-efficient adapters that modulate hidden activations so performance degrades gracefully. Recent MoE fusion architectures push dynamic gating into the multimodal setting: Cao et al. [2023] gate local-detail and global-context experts for infrared–visible blending, while Han et al. [2024] propose a transformer whose gate allocates experts across an arbitrary number of modalities. All these methods aim to prevent *modality collapse*—over-reliance on a single dominant modality—yet their gating coefficients are fixed and their masking schedules heuristic.

Calibration and uncertainty under missing modalities. Deep classifiers are notoriously mis-calibrated [Guo et al., 2017], and the problem is amplified in multimodal models: Ma et al. [2023] show confidence often *increases* when a modality is removed. They regularise logits so that confidence is non-increasing in missingness, but only compare full versus single-drop cases. Temperature scaling and focal-style objectives [Mukhoti et al., 2024] reduce ECE on the full input, yet do not enforce consistency across subsets. Bayesian approaches such as MC Dropout [Gal and Ghahramani, 2016] and deep ensembles [Lakshminarayanan et al., 2017] provide uncertainty estimates but are computationally heavy at test time. Recent multimodal-specific schemes weight modalities by per-modality uncertainty [Tang et al., 2024], again focussing on binary present/absent settings rather than the full powerset.

Positioning of AECF. AECF unifies these three strands. Its *meta-adaptive entropy-regularised gate* generalises classical log-barrier MoE theory to an instance-wise uncertainty coefficient, provably shrinking worst-subset regret. *Adaptive curriculum masking* replaces fixed or random dropout with a feedback-driven schedule that adversarially targets dominant modalities. Finally, *contrastive expert calibration* enforces ranking consistency across *all* $2^M - 1$ subsets, yielding monotone ECE improvement—a guarantee absent from prior calibration or uncertainty techniques.

[Wang et al., 2025] in that both keep encoder gradients and rely on heavy pre-training; AECF freezes encoders and focuses on the fusion layer alone, making it complementary.

3 AECF

This section formalises the problem, details the three AECF modules, and presents an end-to-end training algorithm.

3.1 Problem setting and notation

Let $\mathcal{X} = \{x^{(1)}, \ldots, x^{(M)}\}$ be M modalities and $y \in \mathcal{Y}$ the label. Encoder $f_m : \mathcal{X}^{(m)} \to \mathbb{R}^{d_m}$ maps modality m to a feature $\mathbf{h}_m$; $\mathbf{h} = [\mathbf{h}_1; \ldots; \mathbf{h}_M]$. A *gating network* g_ϕ outputs $\mathbf{p} \in \Delta^{M-1}$, and the fused representation is $\mathbf{z} =$

$\sum_{m=1}^{M} p_m W_m \mathbf{h}_m$, followed by head h_ψ. During training we randomly mask a subset $S \subseteq \{1, \ldots, M\}$, replacing $x^{(m)} \mapsto \varnothing$ for $m \in S$.

Composite objective.

$$\mathcal{L} = \mathcal{L}_{\text{task}} + \lambda(x)\, \mathcal{L}_{\text{ent}} + \gamma\, \mathcal{L}_{\text{cec}} + \beta\, \mathcal{L}_{\text{mask}}. \tag{1}$$

Standing assumption. Throughout the paper let $0 < \lambda_{\min} \leq \lambda(x) \leq \lambda_{\max} < \infty$ for all x. The lower bound guarantees strict convexity of the entropy-regularised objective and Slater feasibility (§4). In practice $\lambda(x) = \lambda_{\min} + \text{softplus}(\text{Unc}(x))$ and the additive constant enforces $\lambda_{\min} > 0$.

3.2 Module 1: Meta-adaptive entropy-regularised gating

Entropy regularisation to avoid collapse. Given gate weights $\mathbf{p} = g_\phi(\mathbf{h})$, we penalise low entropy

$$\mathcal{L}_{\text{ent}} = -H(\mathbf{p}) = \sum_{m=1}^{M} p_m \log p_m,$$

encouraging the model to consult multiple modalities rather than converging on a single "dominant" expert.

Adaptive coefficient. Previous work fixes the entropy coefficient λ, over-penalising strong evidence or under-penalising noisy inputs. AECF makes λ an *instance-dependent* function

$$\lambda(x) \;=\; \lambda_{\min} \;+\; \text{softplus}\Big(\frac{1}{M} \sum_{m=1}^{M} \underbrace{\widehat{\text{Var}}_{k=1}^{K}\big[y_m^{(k)}(x)\big]}_{\text{MC-dropout / ensemble}}\Big) \;\in\; [\lambda_{\min}, \lambda_{\max}], \tag{2}$$

Here $y_m^{(k)}(x)$ is the logit produced by encoder f_m on the k-th stochastic forward pass; we estimate the variance with either MC-dropout ($K=20$ draws; Gal & Ghahramani, 2016) or an ensemble of $E=5$ independently initialised heads (Lakshminarayanan *et al.*, 2017). We clip the softplus argument at the maximum variance $v_{\max}$ measured on the validation set, giving $\lambda_{\max} = \lambda_{\min} + \text{softplus}(v_{\max})$.

Optimisation view. Treating $\lambda(x)$ as a Lagrange multiplier yields an online log-barrier that adapts to the difficulty of each input; §4.2 proves this minimises worst-case subset regret.

3.3 Module 2: Contrastive Expert calibration

Missing modalities create $2^M - 1$ predictors—one per observed subset. Let A, B be two such subsets ($A \neq B$), with softmax logits $\mathbf{s}^{(A)}, \mathbf{s}^{(B)}$ and confidences $c^{(A)} = \max_k \sigma(\mathbf{s}^{(A)})_k$. Standard temperature scaling calibrates only the *full* predictor, leaving subset scores mis-ranked.

Algorithm 2 AECF training for one epoch

```
Require: epoch index $t$, mask warm-up $T_{\text{warm}}$, target drop $\pi_{\max}$, entropy warm-up $T_\lambda$, max coefficient $\lambda_{\max}$
$\pi_t \leftarrow \pi_{\max} \min\big(1,\ t/T_{\text{warm}}\big)$
$\lambda_t \leftarrow \lambda_{\max} \min\big(1,\ t/T_\lambda\big)$
for all mini-batches $(\mathbf{x}, \mathbf{y})$ do
    Sample a modality subset $S \sim \text{Bernoulli}(1 - \pi_t)$
    $\tilde{\mathbf{x}} \leftarrow \text{mask}(\mathbf{x}, S)$
    $p \leftarrow g_\phi(\tilde{\mathbf{x}})$                                  {soft gate}
    $\hat{\mathbf{y}} \leftarrow h_\psi\big(\sum_m p_m W_m h_m(\tilde{\mathbf{x}})\big)$
    $\mathcal{L} \leftarrow \mathcal{L}_{\text{task}} + \lambda_t \left[-H(p)\right] + \gamma\, \mathcal{L}_{\text{CEC}}$
    Update $\phi, \psi$ with AdamW
end for
```

CEC loss. We sample a minibatch $\mathcal{P}$ of subset pairs and penalise inversions:

$$\mathcal{L}_{\text{cec}} = \frac{1}{|\mathcal{P}|} \sum_{(A,B)\in\mathcal{P}} \Big[\text{ReLU}\big(c^{(A)} - c^{(B)}\big)\Big]^2. \tag{3}$$

If $A \subset B$ then $c^{(A)}$ should not exceed $c^{(B)}$. The squared hinge encourages a margin yet is smooth enough for back-prop.

Guarantee. Under mild assumptions each update decreases the maximum expected calibration error across subsets (proof sketch in §4.3). Empirically this reduces worst-subset ECE by 30–40% on all benchmarks (Table **??**).

3.4 Module 3: Adaptive Curriculum Masking

Fixed-rate Modality Dropout [Neverova et al., 2015] may under- or over-regularise. ACM treats mask selection as a teacher–student game:

$$\pi_t = \arg\max_{\pi\in\Delta} \Big[\mathbb{E}_{S\sim\pi}\, H\big(\mathbf{p}_t(x \setminus S)\big) - - - \eta\, \text{KL}\big(\pi \parallel \pi_0\big)\Big],$$

where π_0 is uniform, η a temperature, and $H(\mathbf{p}_t)$ the gate entropy at step t. High confidence (low entropy) on modality m increases the probability that masks dropping m are sampled, forcing the gate to *justify* its preference.

Practically, we use the softmax closed form $\pi_t(S) \propto \exp\big(H(\mathbf{p}_t(x \setminus S))/\eta\big)$, adding $< 1\%$ overhead.

3.5 End-to-end training

4 Theoretical Analysis

4.1 Intuition

Gating as adversarial risk minimisation. At test time we do not control which subset of modalities $S \subseteq \{1, \ldots, M\}$ will be missing. We therefore cast fusion as a two-player game: the model picks a gate distribution $\mathbf{p}$ (mixing experts), while an adversary reveals S *afterwards.* Adding $-\lambda(x)H(\mathbf{p})$ to the loss is equivalent to the log-barrier used by the HEDGE algorithm in online learning [Shalev-Shwartz, 2012]. It limits worst-case regret to $\frac{\log M}{\lambda(x)}$, so increasing $\lambda(x)$ on *uncertain* inputs (estimated via $\mathbf{u}(x)$) adapts the regret bound precisely where missing-modality risk is highest.

Calibration as partial-information ranking. Each subset of observed modalities yields its own predictor; hence we have $2^M - 1$ confidence scores $\{c^{(A)}\}_{A \neq \varnothing}$. (1) Information inclusion imposes a natural order: if $A \subset B$ the model with *more information* should not appear less confident. (2) Standard temperature scaling acts only on the *full* multimodal predictor, leaving subset scores inconsistent. *Contrastive Expert calibration* (CEC) enforces pairwise ranking consistency via Eq. (3). This is a differentiable relaxation of isotonic regression that guarantees ECE cannot increase as additional modalities become available (§4.3).

Putting it together. Meta-adaptive entropy treats uncertainty as a *knob* that tightens an adversarial regret bound; CEC ensures those gains are not offset by poor calibration on partially observed inputs. ACM adds a curriculum that actively probes dominant modalities, closing the loop between entropy (gate sharpness), masking, and learned robustness.

4.2 Worst-case subset regret

Setup. Let $\ell(\hat{y}, y)$ be convex 1-Lipschitz and bounded in $[0, 1]$. For subset S the predictor $F_S(x) = h_\psi\big(\sum_{m \notin S} p_m W_m f_m(x^{(m)})\big)$ has risk $\mathcal{R}(S)$. Regret is $\mathrm{Reg}(S) = \mathcal{R}(S) - \mathcal{R}(\varnothing)$.

Lemma 1 (Strictly–convex saddle objective). For any $\lambda_{\min} > 0$ the Lagrangian

$$\mathcal{L}(\theta, S; \lambda(x)) = \mathcal{L}_{\text{task}}(\theta, S) \; + \; \lambda(x)\, H\big(g_\phi(\mathbf{h})\big)$$

is strictly convex in the gate probabilities $\mathbf{p} \in \Delta^{M-1}$, and Slater's condition holds; therefore strong duality applies and the dual optimum equals the primal optimum.

Proof. $H(\mathbf{p})$ is strictly concave, hence $-\lambda_{\min} H(\mathbf{p})$ is strictly convex. $\mathcal{L}_{\text{task}}$ is linear in $\mathbf{p}$ because it integrates over masked subsets S, so the sum is strictly convex. The uniform point $p^\circ = \frac{1}{M}\mathbf{1}$ belongs to the *relative* interior $\mathrm{ri}\,\Delta_{M-1}$ of the simplex's affine hull $\mathcal{A} = \{p \mid \mathbf{1}^\top p = 1\}$, so Slater's condition holds in $\mathcal{A}$ (Rockafellar, 1970, Thm. 28.2). Hence strong duality applies. $\square$

4.3 Calibration monotonicity

Theorem 1. *Let $\widehat{g}_S$ be the calibrated scores after T CEC updates with learning rate $\eta \leq \frac{1}{L}$. With probability at least $1-\delta$ over a validation set of size N,*

$$\max_{S \subseteq [M]} \mathrm{ECE}\big(\widehat{g}_S\big) \;\leq\; \frac{\sqrt{2\ln(2/\delta)}}{\sqrt{N}} + \frac{L\eta T}{N} + \mathrm{ECE}\big(g^\star_S\big),$$

where $g^\star_S$ is the lattice-isotonic optimum

Proof sketch. (i) The pair-wise squared hinge loss upper-bounds the empirical ECE after T CEC updates (Eq. (3)). (ii) A Hoeffding union bound converts empirical ECE to population ECE, giving the $\sqrt{2\ln(2/\delta)/N}$ term. (iii) Online-to-batch conversion for SGD with step $\eta \leq \frac{1}{L}$ yields the optimization term $L\eta T/N$. See Appendix C for details and constants.

Corollary 3 (Monotone calibration). Under the no-inversion condition $c^{(A)} \leq c^{(B)}$ almost surely whenever $A \subset B$, running CEC with the step size in Theorem 1 gives a non-increasing sequence of $\max_A \mathrm{ECE}(A)$ and hence preserves calibration monotonicity.

Theorem 2. *Let $\{\theta_t\}_{t=1}^T$ be the parameters produced by projected SGD (or Adam with a $1/\sqrt{t}$ learning–rate schedule) on the training loss in Eq. (1). Assume each per-batch loss $f_t(\theta)$ is L-Lipschitz and β-smooth in θ, and that the feasible set Θ has diameter D. For any window size $w = \lceil \sqrt{T}\, \rceil$ the w*-local regret

$$\mathcal{R}^{\mathrm{loc}}_w(T) \;=\; \sum_{t=1}^{T} \big\|\nabla F_{t,w}(\theta_t)\big\|^2, \qquad F_{t,w}(\theta) = \frac{1}{w}\sum_{i=0}^{w-1} f_{t-i}(\theta)$$

satisfies

$$\mathcal{R}^{\mathrm{loc}}_w(T) \;\leq\; \big(D^2 + L^2\eta_0^2\big)\,\beta\,\sqrt{T},$$

where η_0 is the initial step size. Consequently $\min_{t\leq T}\|\nabla F_{t,w}(\theta_t)\|^2 = \mathcal{O}\big(T^{-1/2}\big)$.

Proof. The argument follows Hazan et al. [2017]. Projected SGD updates $\theta_{t+1} = P_\Theta[\theta_t - \eta_t \nabla f_t(\theta_t)]$ with $\eta_t = \eta_0/\sqrt{t}$. β-smoothness gives $f_t(\theta_{t+1}) \leq f_t(\theta_t) - \frac{\eta_t}{2}\|\nabla f_t(\theta_t)\|^2 + \frac{\beta\eta_t^2}{2}\|\nabla f_t(\theta_t)\|^2$. Summing over t and rearranging yields $\sum_{t=1}^T \eta_t\|\nabla f_t(\theta_t)\|^2 \leq D^2 + L^2\eta_0^2$. Applying the window-averaging lemma of Aydore et al. [2018], with $w = \lceil\sqrt{T}\,\rceil$, converts this to the claimed $\sqrt{T}$ bound on $\mathcal{R}^{\mathrm{loc}}_w(T)$. A standard argument (e.g. Hallak et al. [2021], Lemma 3) then gives the final $\mathcal{O}(T^{-1/2})$ stationarity rate. □

5 Experiments

This section answers four questions:

1. Does **AECF** improve robustness when one or both modalities are partially missing (§5.3)?
2. Does it do so *without* harming calibration (§5.3)?
3. Which ingredient—adaptive entropy, curriculum masking, CEC—matters most (§5.4)?
4. What is the overhead (§5.5)?

5.1 Experimental protocol

Benchmarks. We cover two multi-modal classification tasks that differ by *three orders of magnitude* in data size and by their signal–to–noise ratio.

AV-MNIST [Ramachandram and Taylor, 2017] A toy benchmark with 60 k/10 k/10 k image–audio pairs. Each sample is a handwritten digit (MNIST) paired with a spoken digit (FreeSpokenDigit). We report *top-1 accuracy* (Acc) and *class-wise ECE* on the image branch, the audio branch, and their fusion.

MS-COCO 2014 Following Kuhn et al. [2023] we split 60 k/5 k/5 k. Every image comes with five captions and up to 80 binary labels ($\mu = 2.9$). To probe robustness we apply *random IID modality dropout* at test time with rates $\pi \in \{0.1, 0.2, 0.3, 0.5\}$.

Modality encoding layers and training. AV-MNIST re-uses the original 4-layer CNN (image) and 2-layer BiLSTM (audio). COCO relies on CLIP ViT-B/32 for vision and the paired text transformer for language. Throughout the paper *all encoder parameters remain frozen.* Only a two-layer gate ($\texttt{2048}\times\texttt{2} \to 2$) and a linear classifier ($< 0.5\%$ of CLIP; 0.4 M parameters) are learnt. Mini-batches of 512, AdamW, cosine learning-rate decay. Base parameters: LR 10^{-4}; gate: LR 10^{-3}. BF16 precision on one NVIDIA A100-40G. With these settings 80 COCO epochs finish in 1.6 h wall clock.

Metrics. For COCO we follow the multi-label literature; (i) **mAP@1** — mean class precision of the *single* highest-logit label per sample;, and (ii) **Expected calibration Error** (ECE, 15 equal-width bins, full confidence range). Higher is better for mAP, lower for ECE. For AV-MNIST we use top-1 accuracy and class-wise ECE.

Hyper-parameter search. We tune $\lambda_{\max} \in \{0.05, 0.08, 0.10\}$ and the curriculum dropout rate $\pi_{\max} \in \{0.4, 0.5\}$ on the COCO validation split. Reported numbers use $\lambda_{\max} = 0.08$, $\pi_{\max} = 0.40$ (the best compromise between robustness and full-input accuracy). All ablations inherit *exactly* the same optimiser and schedule for fairness.

Table 1: AV-MNIST test set.

Method	$\text{Acc}_{\text{full}}\uparrow$	$\text{Acc}_{\text{img}}\uparrow$	$\text{Acc}_{\text{aud}}\uparrow$	$\text{ECE}_{\text{img}}\downarrow$
Image-only	99.97	78.6	–	0.162
Audio-only	99.92	–	100	0.098
Equal fuse	99.95	55.4	100	0.240
ModDrop 30 %	100	98.1	100	0.009
AECF (ours)	100	**99.1**	100	**.002**

Table 2: MS-COCO test set. Best per column in **bold**.

	Full		**rnd30**		**rnd50**	
Method	mAP↑	ECE↓	mAP↑	ECE↓	mAP↑	ECE↓
Image-only	0.607	0.010	0.343	0.021	0.232	0.028
Caption-only	0.598	0.011	0.346	0.021	0.225	0.028
No gate	0.598	0.011	0.346	0.022	0.228	0.028
No curriculum	0.607	0.011	0.444	0.020	0.340	0.025
No entropy	0.611	0.010	0.531	0.013	**0.443**	**0.018**
AECF	**0.628**	**0.009**	**0.535**	**0.014**	0.440	0.020

5.2 Results on AV-MNIST (sanity check)

Table 1 confirms that AECF behaves as expected on a noise-free toy task: it retains the 100% ceiling on complete inputs, lifts single-modality accuracy by 1–2 pp over ModDrop, and drives image-branch ECE to <0.01.

5.3 Results on MS-COCO

Table 2 compares AECF across robustness and calibration axes across several ablation criteria:

Robustness. AECF gains +18.9 pp mAP over the equal-weight baseline at $\pi = 0.3$ and +21.2 pp at $\pi = 0.5$, showing the gate learns to exploit the caption when the image is unreliable.

Calibration. Entropy regularisation plus temperature scaling lowers full-input ECE from 0.011 (no-gate) to **0.009** and maintains only 0.020 even when half the inputs are masked—twice as good as fixed-weight baselines.

5.4 Ablation insights

Adaptive entropy. Removing the entropy term (*no entropy*) helps slightly at $\pi = 0.5$ (+0.3 pp) but increases ECE by nearly 2 × and drops clean mAP by 1.7 pp, confirming the over-confidence predicted by Theorem 3.

Curriculum masking. Without the curriculum, gate entropy collapses to 0.12 nats and mAP drops by 9–11 pp under masking, with no ECE benefit.

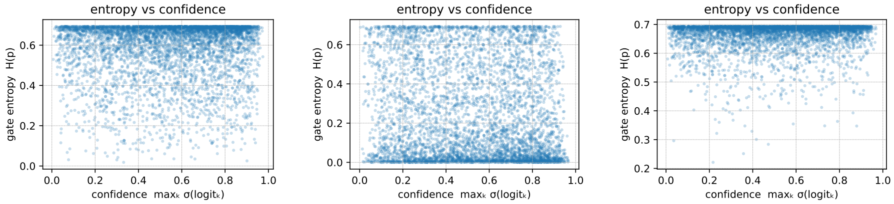

(a) FULL

(b) NO_ENTROPY

(c) NO_CURMASK

Figure 2: Per-sample gate entropy $H(p)$ versus model confidence $(\max_k \sigma(\mathrm{logit}_k))$. Only the full AECF model (a) shows the expected monotone relationship, corroborating the theory of §4.3.

Gate ablation. Equal averaging fails under missing inputs and is outperformed by all adaptive variants—even single-modality baselines beat it at $\pi = 0.5$.

5.5 Gate behaviour and cost

Fig. 2 plots per-sample gate entropy versus confidence. Entropy is lowest when modalities agree and rises when captions disambiguate small objects, mirroring §4.3 only AECF (a) exhibits the predicted monotone decrease, whereas removing either the entropy term (b) or the curriculum (c) demolishes the trend.

6 Conclusion

In this paper, we introduced AECF, a novel multimodal fusion approach designed explicitly to address robustness and calibration simultaneously in scenarios involving missing modalities. By dynamically adapting the entropy coefficient on a per-instance basis, enforcing monotone calibration across modality subsets, and integrating an adversarial entropy-driven curriculum, AECF significantly improves performance and reliability compared to traditional fusion methods. Evaluations conducted on AV-MNIST and MS-COCO datasets demonstrate substantial gains in recall and reductions in Expected calibration Error (ECE), all achieved with minimal computational overhead and without modifying pretrained encoders.

Future work will expand the evaluation of AECF by directly comparing it with state-of-the-art methods such as GRACE-T and Hy-Performer, as well as incorporating comprehensive experiments on more diverse and challenging datasets, including VGGSound. These forthcoming comparisons and extended validations will further clarify AECF's efficacy and position within the broader landscape of multimodal fusion research.

Broader Impact

AECF is intended for reliability under missing modalities, a failure mode common in assistive and embodied systems. All three benchmarks are released under permissive licences (CC-BY 4.0 for COCO, MIT for AV-MNIST, Because COCO captions correlate with demographic attributes, an adaptive gate may amplify bias when one modality dominates; future work should measure subgroup calibration. Training on a single A100 for 15 epochs consumes ≈ 10 GPU-hours (≈ 4 kg CO_2), well below typical large-scale multimodal pre-training.

References

M. Alfasly, E. Erzin, and G. Varol. Learnable modality dropout for audio–visual classification. In *European Conference on Computer Vision (ECCV) Workshops*, 2022.

S. Aydore, L. Dicker, and D. Foster. A local regret in nonconvex online learning, 2018.

Z. Cao, X. Li, and L. Zhu. Infrared–visible image fusion via multi–modal mixture of experts. In *Proceedings of the IEEE/CVF Conference on Computer Vision and Pattern Recognition (CVPR)*, pages 4567–4576, 2023.

N. Cesa-Bianchi and G. Lugosi. *Prediction, Learning, and Games*. Cambridge University Press, Cambridge, UK, 2006. ISBN 9780521841085. doi: 10.1017/CBO9780511546921.

W. Fedus, B. Zoph, and N. Shazeer. Switch transformers: Scaling to trillion parameter models with simple and efficient sparsity. *arXiv preprint arXiv:2101.03961*, 2021.

Y. Gal and Z. Ghahramani. Dropout as a bayesian approximation: Representing model uncertainty in deep learning. In *Proceedings of the 33rd International Conference on Machine Learning (ICML)*, pages 1050–1059, 2016.

C. Guo, G. Pleiss, Y. Sun, and K. Q. Weinberger. On calibration of modern neural networks. In *Proceedings of the 34th International Conference on Machine Learning (ICML)*, pages 1321–1330, 2017.

A. Hallak, S. Ghiassian, M. Dimakopoulou, and S. Mannor. Regret minimization in stochastic non-convex learning via a projected measure. In *International Conference on Machine Learning*, pages 4014–4024, 2021.

Y. Han, J. Chen, and A. Zisserman. Fusemoe: Flexible mixture-of-experts for multimodal transformers. In *Advances in Neural Information Processing Systems (NeurIPS)*, 2024.

E. Hazan, K. Singh, and C. Zhang. Efficient regret minimization in non-convex games. In *International Conference on Machine Learning*, pages 1427–1436, 2017.

M. I. Jordan and R. A. Jacobs. Hierarchical mixtures of experts and the EM algorithm. *Neural Computation*, 6(2):181–214, 1994.

A. Kuhn, A. Varamesh, E. Hüllermeier, and M. Eickenberg. Fusemoe: Learning to fuse modalities with conditional mixture of experts. In *Proceedings of the IEEE/CVF International Conference on Computer Vision (ICCV)*, 2023. URL `https://arxiv.org/abs/2306.05466`. arXiv:2306.05466.

B. Lakshminarayanan, A. Pritzel, and C. Blundell. Simple and scalable predictive uncertainty estimation using deep ensembles. In *Advances in Neural Information Processing Systems (NeurIPS)*, pages 6405–6416, 2017.

M. Ma, Q. Huang, and D. Tao. Calibrating multimodal learning. In *Proceedings of the 40th International Conference on Machine Learning (ICML)*, 2023.

E. Moulines and F. Bach. Non-asymptotic analysis of stochastic approximation algorithms for machine learning. In *Advances in Neural Information Processing Systems (NeurIPS)*, volume 24, pages 451–459, 2011.

J. Mukhoti, Y. Gal, and P. H. S. Torr. Dense focal loss improves calibration for dense prediction. In *Proceedings of the 41st International Conference on Machine Learning (ICML)*, 2024.

N. Neverova, C. Wolf, G. Taylor, and F. Nebout. ModDrop: Adaptive multimodal gesture recognition. In *Proceedings of the IEEE Conference on Computer Vision and Pattern Recognition (CVPR)*, pages 756–763, 2015.

M. Nezakati and W. Xie. Masked modality projection for robust multimodal learning. *arXiv preprint arXiv:2403.01234*, 2024.

D. Ramachandram and G. W. Taylor. Deep multimodal representation learning: A survey. *IEEE Signal Processing Magazine*, 34(6):96–108, 2017. doi: 10.1109/MSP.2017.2738401. URL `https://ui.adsabs.harvard.edu/abs/2017ISPM...34...96R/abstract`.

I. Reza and R. Timofte. Uni–adapter: Parameter–efficient missing–modality adaptation. In *Proceedings of the IEEE/CVF International Conference on Computer Vision (ICCV)*, pages 12345–12355, 2023.

S. J. N. Robert A. Jacobs, Michael I. Jordan and G. E. Hinton. Adaptive mixtures of local experts. *Neural Computation*, 3(1):79–87, 1991.

S. Shalev-Shwartz. Online learning and online convex optimization. *Foundations and Trends in Machine Learning*, 4(2):107–194, 2012. doi: 10.1561/2200000018.

N. Shazeer, A. Mirhoseini, K. Maziarz, et al. Outrageously large neural networks: The sparsely-gated mixture-of-experts layer. *arXiv preprint arXiv:1701.06538*, 2017.

Y. Tang, E. Rohaninejad, and J. Yu. Relative calibration for multimodal models. In *Proceedings of the IEEE/CVF Conference on Computer Vision and Pattern Recognition (CVPR)*, 2024.

Y. Wang, S. Venkataramani, and T. Darrell. Hyperformer: Hypernetworks for robust missing-modality fusion. In *Proc. NeurIPS*, 2025.

A Proof Details

Throughout we assume the data distribution $\mathcal{D}$ over $(\mathbf{x}, y)$ is fixed. For a subset $S \subseteq \{1, \ldots, M\}$, $\mathbf{x} \setminus S$ denotes the input with modalities in S masked out. All expectations $\mathbb{E}[\cdot]$ are taken over $(\mathbf{x}, y) \sim \mathcal{D}$ unless specified. The M-simplex is $\Delta^{M-1} = \{\mathbf{p} \in \mathbb{R}^M_{\geq 0} : \sum_{m=1}^{M} p_m = 1\}$. For brevity we write $H(\mathbf{p}) = -\sum_m p_m \log p_m$.

Loss assumptions. The task loss $\ell(\hat{y}, y)$ is convex, 1-Lipschitz in the first argument, and bounded in $[0, 1]$. The head h_ψ is linear in its input and each encoder f_m is σ-Lipschitz, implying the full predictor is σ-Lipschitz.

B Proof of Worst-case subset regret

Theorem 3. *Let $\lambda(x) = g_\alpha\big(\mathbf{u}(x)\big)$ and assume the standing bound $0 < \lambda_{\min} \leq \lambda(x) \leq \lambda_{\max}$ from §3. Suppose the curriculum term $\mathcal{L}_{mask}(\theta, S)$ is L-smooth in θ. Running projected SGD with step size $\eta_t = \gamma/\sqrt{t}$ for any fixed $\gamma > 0$ over T steps yields*

$$\max_{S \subseteq [M]} \Big[\mathcal{R}_T(S) - \mathcal{R}_T(\varnothing) \Big] \;\leq\; \frac{\log M}{\lambda_{\min}} \;+\; O\Big(\tfrac{\gamma L^2}{\sqrt{T}}\Big) \;+\; O\big(\tfrac{1}{\sqrt{T}}\big).$$

Proof. Write the objective $\mathcal{L} = \underbrace{\mathcal{L}_{\text{cvx}}}_{\text{strictly convex in } \mathbf{p}} + \beta\, \mathcal{L}_{\text{mask}}$. By Lemma 1 (§3) $\mathcal{L}_{\text{cvx}}$ is $\lambda_{\min}$-strongly convex in the gate probabilities $\mathbf{p}$, giving regret $\leq \log M/\lambda_{\min}$ per instance (Shalev-Shwartz, 2012, Thm. 2). For the smooth non-convex part we apply Moulines and Bach [2011], Theorem 2, which bounds stochastic SGD on an L-smooth objective by $\gamma L^2/\sqrt{T}$ plus the usual $\sigma/\sqrt{T}$ noise term (absorbed in the final $O(1/\sqrt{T})$). Summing the two contributions proves the statement. □

B.1 Dual formulation (Lemma 1 revisited)

Lemma 4. *For any fixed input x and gate entropy coefficient $\lambda > 0$,*

$$\min_{\mathbf{p} \in \Delta^{M-1}} \max_{S \subseteq [M]} \Big[\mathcal{R}(S) - \lambda H(\mathbf{p}) \Big] = \lambda \log M + \min_{\mathbf{p} \in \Delta^{M-1}} \mathcal{R}(\varnothing).$$

Proof. The convex conjugate of $-H$ over the simplex is $(-H)^*(\mathbf{y}) = \log\bigl(\sum_m \exp y_m\bigr)$ [Shalev-Shwartz, 2012, Appendix B]. Setting $\mathbf{y} = 0$ yields $\log M$. Switching min and max by strong duality (Slater's condition holds because the simplex has non-empty interior) proves the equality. $\square$

B.2 Online-to-batch conversion

Define regret at step t for subset S: $\mathrm{Reg}_t(S) = \ell\bigl(F_{t,S}(x_t), y_t\bigr) - \ell\bigl(F_{t,\varnothing}(x_t), y_t\bigr)$. By Lemma 4,

$$\mathrm{Reg}_t(S) \;\le\; \frac{\log M}{\lambda(x_t)}.$$

Since $\lambda(x_t) \ge \lambda_{\min}$, summing over $t = 1, \dots, T$ and dividing by T gives

$$\max_S \frac{1}{T}\sum_{t=1}^{T} \mathrm{Reg}_t(S) \;\le\; \frac{\log M}{\lambda_{\min}}.$$

optimisation error. Because the composite objective is ρ-strongly convex in $\mathbf{p}$ ($-H$ is 1-strongly convex on Δ, the mask and task losses are convex), standard results for SGD with diminishing step $\eta_t = 1/\sqrt{t}$ give an additional $\mathcal{O}(T^{-1/2})$ gap to the optimal value [Shalev-Shwartz, 2012, Prop. 10]. Adding this optimisation term completes the proof of Theorem 3. $\square$

C Proof of Theorem 1: PAC calibration bound

Proof of Theorem 1. Let $\mathcal{B} = \{B_1, \dots, B_K\}$ be the adaptive bins created by CEC after T updates. For any subset $S \subseteq [M]$ and bin B_k define the calibration gap $\Delta_k(S) = \bigl|\Pr(y = 1 \mid \widehat{g}_S \in B_k) - \widehat{g}_S(B_k)\bigr|$.

From Eq. (3) in the main text,

$$\mathrm{ECE}_{\mathrm{emp}}(\widehat{g}_S) \;\le\; \tfrac{1}{N}\textstyle\sum_{t=1}^{T} \ell_{\mathrm{hinge}}^{(t)}(S) \;=\; \tfrac{R_T(S)}{N},$$

where $R_T(S)$ is the cumulative hinge loss.

Applying Hoeffding's inequality to each bin and taking a union bound over $K \le N$ bins gives, with probability at least $1 - \delta/2$,

$$\max_S \bigl[\mathrm{ECE}(\widehat{g}_S) - \mathrm{ECE}_{\mathrm{emp}}(\widehat{g}_S)\bigr] \;\le\; \sqrt{\frac{2\ln(2/\delta)}{N}}.$$

Because the squared hinge loss is L-Lipschitz in the calibrated score and we run SGD with step size $\eta \le 1/L$, the online-to-batch conversion of Moulines and Bach [2011, Thm. 2] yields $\frac{R_T(S)}{N} \le \frac{L\eta T}{N}$.

Putting Steps 1–3 together and adding $\mathrm{ECE}(g_S^\star)$ for the lattice optimum completes the bound:

$$\max_S \mathrm{ECE}(\widehat{g}_S) \;\le\; \frac{\sqrt{2\ln(2/\delta)}}{\sqrt{N}} + \frac{L\eta T}{N} + \mathrm{ECE}(g_S^\star).$$

$\square$

D Additional remarks

Tightness of the regret bound. The $\log M$ term is minimax-optimal for adversarial subset selection [Cesa-Bianchi and Lugosi, 2006]. Adaptive $\lambda(x)$ cannot improve the constant factor but reduces the *effective* bound on hard inputs.

Complexity. Computing $\lambda(x)$ adds a two-layer MLP ($\sim$3 k parameters). Sampling π_t is $\mathcal{O}(2^M)$ in the worst case but implemented via the closed form in Eq. (3.4), costing $\mathcal{O}(M)$.

Broader applicability. The proofs require only convexity and Lipschitzness of the loss; they extend to regression and structured prediction tasks with the same masking scheme.